IABSE-JSCE Joint Conference on Advances in Bridge Engineering-IV, August 26-27, 2020, Dhaka, Bangladesh
Amin, Okui, Bhuiyan, Rahman (eds.)
ISBN: 978-984-34-8313-3
www.iabse-bd.org

Displacement estimation of nonlinear SDOF system under seismic excitation using Kalman filter and parameter optimization

Y. Yang, T. Nagayama, K. Ishihara & D. Su
The University of Tokyo, Bunkyo-ku 113-0027, Tokyo, Japan

ABSTRACT: A displacement estimation method for nonlinear SDOF system under seismic excitation is proposed based on Extended Kalman filter (EKF) and parameter optimization. Time interval where system experiences significant nonlinearity or not is firstly distinguished. For time period when system is in elastic phase, available observations for EKF are acceleration, double integrated displacement and residual displacement value. During time period with significant nonlinearity, acceleration is only employed as observation and a bi-linear hysteresis model is assumed in this part to estimate displacement using EKF. The results are further smoothed by Extended Kalman smoother (EKS). The proposed method is numerically verified using a SDOF system with bi-linear hysteresis model and further validated through an E-defense experiment. The estimated displacements from both numerical examples and experiment present good accuracies.

1 INTRODUCTION

Displacement response is an important indicator reflecting structural health condition after an earthquake excitation. For example, inter-story drift ratio (IDR) (Shodja et al. 2014)), defined as inter-story drift normalized by story height is used as judgment criterion on buildings; hysteresis loop of a SDOF system which can be presented as displacement versus inertial force, contains energy dissipation information of the system (Kuleli 2018). Besides, in the context of system identification, displacement measurements are preferred because consistent stiffness identification results may not be easily obtained by observing only accelerations as reported by Chatzis et al. 2015. Generally, displacement measurements would be more beneficial in the field of structural health monitoring (SHM).

Measuring structural displacement is usually a challenging task in practice. Since displacement is a relative physical quantity, a stationary platform is needed for contact displacement sensors, e.g. LVDT. The sensors might work well in indoor environment, but difficulty in finding reliable platform can become a significant obstacle for on-site applications. Non-contact technologies, such as global positioning systems (GPS), are alternatives. However, drawbacks of most of them include but not limited to high equipment cost, low sampling frequency, and low resolution. A comprehensive review of various inter-story displacement measurement techniques is found in (Skolnik et al. 2010). Compared to displacement transducer, accelerometer is preferable in practice considering its advantages such as high sampling frequency, robustness, and ease of deployment. By double integrating acceleration signals and applying baseline correction and appropriate high pass filter, reasonable displacement can be obtained (Yang et al. 2006). Besides, novel displacement estimation methods using acceleration measurement have been developed (Lee et al. 2010) and applied to wireless displacement measurement system (Park et al. 2013). The acceleration integration based methods perform well in terms of linear system case, e.g. within 1%~ 4% errors at peak displacement prediction in inter-story drift as reported in (Skolnik et al. 2010). However, due to the effect of high pass filter, they cannot be applied to system undergoing nonlinear deformations since low frequency drift component including residual displacement are inevitably removed.

In this paper, an Extended Kalman filter (EKF) based displacement estimation method is proposed for nonlinear SDOF system under seismic excitation. Acceleration and residual displacement are utilized. From a forward simulation point of view, residual displacement is sensitive to nonlinear system parameters, e.g. post-yielding stiffness ratio α in bi-linear model studied by Kawashima et al. 1998. It indicates that estimation of residual displacement may not be implemented easily in practice. Therefore, the residual displacement is as-

sumed as known in this study, which could be obtained from inclinometers in practice (Nagayama et al. 2017).

In the proposed method, firstly, time-intervals of responses with and without significant system nonlinearity are distinguished based on a time-variant parameter estimation method (Kuleli et al. 2020). For time period without nonlinearity, e.g. the beginning and end parts of time history, observations in EKF include acceleration and displacement which is obtained by combining double integrated and high pass-filtered displacement and residual displacement. During time interval with significant nonlinearity, only acceleration is used as measurement. In order to consider the nonlinearity, a bi-linear hysteresis model is assumed and its model parameters are optimized by genetic algorithm (GA). The result from EKF is further smoothed by Extended Kalman smoother(EKS). In following, the displacement estimation method is presented in section 2 in detail. In section 3, the proposed method is numerically verified with a SDOF system with bi-linear hysteresis model. In section 4, a bridge pier shaking table experiment from E-defense database is used to validate the method. Finally, conclusion is given in section 5.

2 DISPLACEMENT ESTIMATION METHOD

2.1 *Equation of Motion and State Space Model*

The equation of motion (EOM) of a nonlinear SDOF system under seismic excitation in relative coordinate is written as

$$m\ddot{x} + c\dot{x} + f\left(x, \dot{x}\right) = -m\ddot{u}_g \tag{1}$$

in which x , $\dot{x}$ and $\ddot{x}$ are vectors of displacement, velocity and acceleration respectively; m and $c$are mass and damping coefficient; f represents nonlinear restoring force as a function of x and $\dot{x}$, and determines hysteresis rule of loading and unloading; $\ddot{u}_g$ is input ground acceleration. The incremental formulation is written as

$$m\Delta\ddot{x} + c\Delta\dot{x} + k_T\Delta x = -m\Delta\ddot{u}_g \tag{2}$$

in which Δ stands for incremental value and k_T is tangential stiffness for each time instance. Usually, equation (2) is solved by numerical integration algorithm in a step by step manner; using incremental New mark-β method, the equation is transformed into a discrete state space model as

$$\begin{bmatrix} x(k+1) \\ \dot{x}(k+1) \\ \ddot{x}(k+1) \end{bmatrix} = \left\{ \boldsymbol{I} + \begin{bmatrix} 1 \\ \delta/\beta\Delta t \\ 1/\beta\Delta t^2 \end{bmatrix} \boldsymbol{L} + \begin{bmatrix} 0 & 0 & 0 \\ 0 & -\delta/\beta & \left(1-\delta/2\beta\right)\Delta t \\ 0 & -1/\beta\Delta t & -1/2\beta \end{bmatrix} \right\} \begin{bmatrix} x(k) \\ \dot{x}(k) \\ \ddot{x}(k) \end{bmatrix} + \begin{bmatrix} 1 \\ \delta/\beta\Delta t \\ 1/\beta\Delta t^2 \end{bmatrix} k_d^{-1} m\Delta\ddot{u}_g \tag{3}$$

in which β and δ are integration parameters of the algorithm which are set as 1/6 and 1/2 in this study; $\boldsymbol{I}$ is the unit matrix; k stands for a specific time instant, $\boldsymbol{L}$ matrix is defined as below

$$\boldsymbol{L} = \left\{ 0 \quad k_d^{-1}\left(\frac{m}{\beta\Delta t} + \frac{\delta c}{\beta} \right) \quad k_d^{-1}\left[\frac{m}{2\beta} + c\left(\frac{\delta}{2\beta} - 1 \right)\Delta t \right] \right\} \tag{4}$$

k_d is equivalent dynamic stiffness which is calculated as

$$k_d = \frac{1}{\beta\Delta t^2} m + \frac{\delta}{\beta\Delta t} c + k_T \tag{5}$$

This state space model is different from commonly used one where only displacement and velocity variables are included in the state vector. In the commonly used state space model, dynamic equilibrium is exerted implicitly on every point according to its integration algorithm. Because of that, the state space model can only estimate displacements of a linear elastic system. However, dynamic equilibrium is not enforced in the state space model of equation (3), thus it can be applied to displacement estimation of a nonlinear system.

In this study, if necessary, parameters can also be identified by augmenting them in the state vector. Specifically, the augmented state vector, system equation, and observation equation in EKF are written as

$$\boldsymbol{X}_a = \left[\boldsymbol{x}(t)^T \quad \dot{\boldsymbol{x}}(t)^T \quad \ddot{\boldsymbol{x}}(t)^T \quad \boldsymbol{\theta}^T \right]^T \tag{6}$$

$$\boldsymbol{X}_a(k+1) = \boldsymbol{f}\left(\boldsymbol{X}_a(k), \Delta\ddot{u}_g \right) + \boldsymbol{w}(k) \tag{7}$$

$$\boldsymbol{y}(k+1)=\boldsymbol{h}\left(\boldsymbol{X}_a(k+1)\right)+\boldsymbol{v}(k+1) \tag{8}$$

f function is basically the extension of equation (3) with parameters augmented; *h* can be a simple selection matrix containing only 0 or 1; *w*(*k*) and *v*(*k*) are process and measurement noise vector consisting of uncorrelated zero mean noise.

Suppose $\hat{\boldsymbol{X}}_a(k/k)$ and $\boldsymbol{P}(k/k)$ are estimated value and error covariance matrix of state vector at *k* instant based on measurements from 1 to *k* instants. The EKF firstly calculates a prior estimation and covariance matrix of state vector at *k*+1 instant based on system equation (7).

$$\hat{\boldsymbol{X}}_a(k+1/k)=\boldsymbol{f}\left(\hat{\boldsymbol{X}}_a(k/k),\Delta\ddot{u}_g\right) \tag{9}$$

$$\boldsymbol{P}(k+1/k)=\boldsymbol{F}(k)\boldsymbol{P}(k/k)\boldsymbol{F}^T(k)+\boldsymbol{Q}(k) \tag{10}$$

Combining the information from observation equation(8), the estimation and covariance matrix of state vector at *k*+1 instant can be obtained

$$\hat{\boldsymbol{X}}_a(k+1/k+1)=\hat{\boldsymbol{X}}_a(k+1/k)+\boldsymbol{G}\left[\boldsymbol{y}(k+1)-\boldsymbol{h}\left(\hat{\boldsymbol{X}}_a(k+1/k),\Delta\ddot{u}_g\right)\right] \tag{11}$$

$$\boldsymbol{P}(k+1/k+1)=\boldsymbol{P}(k+1/k)-\boldsymbol{G}(k)\boldsymbol{P}_y(k+1/k)\boldsymbol{G}(k)^T \tag{12}$$

In the formulation above, *G*(*k*) is the so called Kalman filter gain matrix and $P_y(k+1/k)$ is prior estimation of observation covariance matrix

$$\boldsymbol{G}(k)=\boldsymbol{P}(k+1/k)\boldsymbol{H}^T(k+1)/\boldsymbol{P}_y(k+1/k) \tag{13}$$

$$\boldsymbol{P}_y(k+1/k)=\boldsymbol{H}(k+1)\boldsymbol{P}(k+1/k)\boldsymbol{H}^T(k+1)+\boldsymbol{R}(k+1) \tag{14}$$

F(*k*) and *H*(*k*+1) are Jacobian matrices of function *f* and *h* respectively

$$\boldsymbol{F}(k)=\left.\frac{\partial\boldsymbol{f}\left(\boldsymbol{X}_a,\ddot{\boldsymbol{u}}_g\right)}{\partial\boldsymbol{X}_a}\right|_{\boldsymbol{X}_a=\hat{\boldsymbol{X}}_a(k/k)} \qquad \boldsymbol{H}(k+1)=\left.\frac{\partial\boldsymbol{h}\left(\boldsymbol{X}_a,\ddot{\boldsymbol{u}}_g\right)}{\partial\boldsymbol{X}_a}\right|_{\boldsymbol{X}_a=\hat{\boldsymbol{X}}_a(k+1/k)} \tag{15}$$

Q(*k*) and *R*(*k*+1) are the process and measurement noise covariance matrices respectively

$$\boldsymbol{Q}(k)=E\left[\boldsymbol{w}(k)\boldsymbol{w}(k)^T\right] \quad \boldsymbol{R}(k+1)=E\left[v(k+1)\boldsymbol{v}(k+1)^T\right]$$

The aforementioned procedures are conducted recursively, regarding estimation of previous instant as initial value for current instant.

2.2 *RM Algorithm for Process Noise Adaption*

The *R* matrix in equation 16 can be decided beforehand, because it is usually related to sensor noise. As for *Q* matrix which actually reflects error of system equation (7) in EKF, a trial and error manner is usually used to tune the value which is time-consuming and subjective. Robbins-Monro stochastic approximation method is originally an algorithm to find root of function which may not be computed directly but estimated from noisy observations (Robbins et al. 1951). Estimation of *Q* matrix using RM method can be formulated as below

$$\boldsymbol{Q}(k+1)=\left(1-\alpha_Q\right)\boldsymbol{Q}(k)+\alpha_Q\boldsymbol{d}(k+1)\boldsymbol{d}(k+1)^T \tag{16}$$

$$\boldsymbol{d}(k+1)=\hat{\boldsymbol{X}}_a(k+1/k+1)-\hat{\boldsymbol{X}}_a(k+1/k) \tag{17}$$

in which *Q*(*k*+1) and *Q*(*k*) are the process noise covariance matrix of next step and current step respectively; *d*(*k*+1) is the so called state innovation vector. The *Q*(*k*+1) matrix is further constrained to have a diagonal form assuming the process noise is uncorrelated. α_Q is a small positive value chosen between 0 and 1, served as a forgetting factor to average estimation of *Q* over a period of time.

Based on the RM algorithm, time-variant parameters can be identified as reported in Kuleli et al. 2020. In the following, the combination of EKF and RM algorithm is referred as EKF-RM method.

2.3 *Observation Scheme*

Accelerations are, in practice, the most easily accessible system responses. Based on acceleration measurement, displacement without low frequency drift can be obtained by double integration and high-pass filtering. Therefore, the true displacement can be obtained as the combination of double integrated displacement and a low frequency drift component. Figure 1 shows the displacement decomposition.

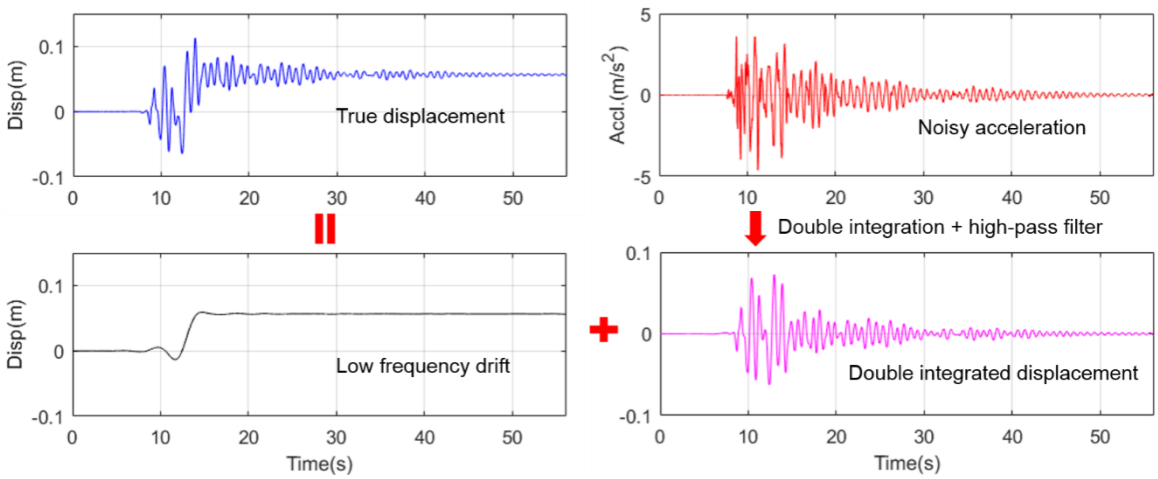

Figure 1. Displacement decomposition.

Because the system under earthquake behave as a linear system when the excitation level is small at the beginning and end of the excitation, double integrated displacement can reproduce the true displacement in these linear sections except for the constant component, i.e. residual displacement component. In the middle part, e.g. 10~20s in the figure above, because of employment of high-pass filter, double integrated displacement differs from the true one significantly.

The residual displacement in this study is assumed as known value; in practice, it can be estimated by inclinometer indirectly. Therefore, the available observation information for displacement estimation includes displacement values at the beginning and end and acceleration signal. The displacements in the linear ranges are obtained by combining double integrated displacement and initial and residual displacement. In order to estimate the nonlinear part of displacement, a virtual displacement observation as shown in Figure 2, i.e. a straight line connecting the two sides, is assumed. The virtual displacement possesses large uncertainties due to the assumption. This method was firstly proposed by Chatzi et al. 2015 for linear displacement estimation using only acceleration to suppress displacement divergence. Figure 2shows the available observation information in the following steps of EKF and EKS.

One remaining problem is how to define the time interval where the virtual displacement should be applied. This time interval is determined by identifying the time-variant parameters k and c of the system based on EKF-RM method using double integrated displacement. Note that the commonly used state space model rather than the incremental New mark-β state space model explained in equation (3) is employed in the EKF-RM method in this parameter identification. While the parameters may not be very accurate especially during the strong nonlinearity part, the time interval with significant stiffness reduction is defined as the part of virtual displacement observation. It will be demonstrated with a numerical example in the following section.

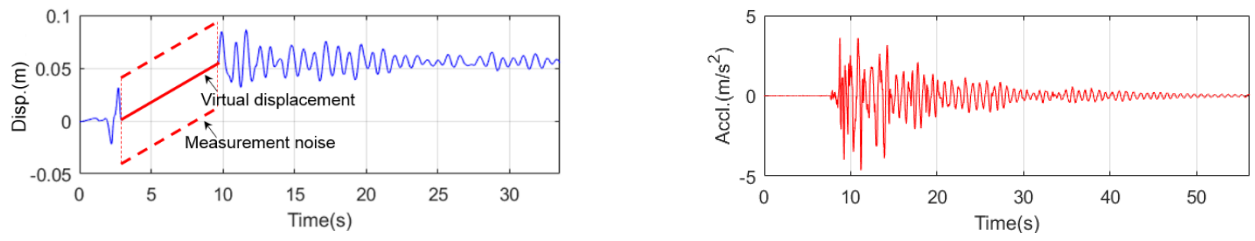

(a) (b)

Figure 2. Available observations (a) displacement (b) acceleration.

2.4 *Estimation Scheme during Virtual Displacement Observation Part*

In order to consider the nonlinearity during the virtual displacement part, a specific hysteresis model is assumed, e.g. bi-linear model. If, in ideal case, the hysteresis model and its corresponding parameters are accurate, displacement can be accurately estimated using ground acceleration measurement only. In case the assumed hysteresis model is different from the real model, an approximate one can be obtained by optimizing parameters of the assumed hysteresis model. In this study, bi-linear model is employed because the model possesses only a few model parameters making the optimization practical. In terms of the elastic stiffness k and damping factor c, appropriate values can be determined from previous step, i.e. when time interval with virtual displacement is defined. Specifically, the identified value in the ending part, i.e. elastic phase, can be used. Therefore, only yielding displacement dy and post-yielding stiffness ratio α need to be obtained. The following fitness function is proposed to optimize these parameters:

$$F_{fitness}(dy,\alpha)=\left(\frac{1}{k_{t1}-k_{t0}+1}\right)\sum_{k=k_{t0}}^{k_{t1}}Q_{accl}\left(k\middle|dy,\alpha\right) \tag{18}$$

in which Q_{accl} stands for acceleration process noise variance at the time instant k given parameters dy and α; k_{t0} and $k_{t1}$are the time steps at the start and end of the virtual displacement. Thus, the basic idea is to find appropriate parameters by minimizing the acceleration process noise variance which indicates model error. The EKF-RM method is applied and the acceleration process noise is obtained. With the optimized parameters, displacement is finally estimated using the EKF-RM method again.

The differences between EKF-RM method used here from one used in determining virtual displacement interval include: 1) the incremental New mark-β state vector is employed in EKF-RM method here while non-incremental state vector is applied to determine virtual displacement interval; 2) the incremental New mark-β state vector contains system responses only, i.e. dy and α parameters are decoupled and not identified along with responses while parameters, i.e. k and c, are included in the state vector when the virtual displacement period is determined.

2.5 *Extended Kalman Smoother*

As mentioned in the last section, $\hat{\boldsymbol{X}}_a(k/k)$ is the estimated value of state vector based on measurement information up to k instant, i.e. $\boldsymbol{y}_{1\sim k}$. In order to utilize measurements of all time instants, especially the signals in the latter parts including residual displacement, EKS based on Rauch-Tung-Striebel smoothing (Rauch et al. 1965)is applied to the outcome of EKF. With the estimated values and error-covariance of state vector at the ending point, i.e. $\hat{\boldsymbol{X}}_a(N/N)$ and $\boldsymbol{P}(N/N)$, the output of the smoother at k instant (k=N-1, N-2,…, 1) is written as

$$\boldsymbol{J}_{k-1}=\boldsymbol{P}(k-1/k-1)\boldsymbol{F}^T(k)\big/\boldsymbol{P}(k/k-1) \tag{19}$$

$$\hat{\boldsymbol{X}}_a(k-1/N)=\hat{\boldsymbol{X}}_a(k-1/k-1)+\boldsymbol{J}_{k-1}\left[\hat{\boldsymbol{X}}_a(k/N)-\hat{\boldsymbol{X}}_a(k/k-1)\right] \tag{20}$$

$$\boldsymbol{P}(k-1/N)=\boldsymbol{P}(k-1/k-1)+\boldsymbol{J}_{k-1}\left[\boldsymbol{P}(k/N)-\boldsymbol{P}(k/k-1)\right]\boldsymbol{J}^T{}_{k-1} \tag{21}$$

in which N stands for the total number of time samples; $\boldsymbol{J}$ is gain matrix of the Kalman smoother; all other symbols are the same as those in section 2.1.

Smoother outputs are more accurate than those from the filter, as shown in the following. Thus after applying EKF-RM method, the estimated result is further smoothed by EKS. Overall, Figure 3 shows the flow chart of the displacement estimation method.

3 NUMERICAL VERIFICATION OF THE DISPLACEMENT ESTIMATION METHOD

The illustrative model considered here is a SDOF system with bi-linear hysteresis model. The prototype of the model is simplified from a full scale bridge pier experiment, called C-1-1 experiment in E-defense shaking database (ASEBI 2020), as shown in the figure below. The basic parameters of the SDOF model includes mass m=252.5 ton, elastic stiffness k=1.625×107 N/m, damping coefficient c=4.05×104 Ns/m, post-yielding stiffness ratio α=0.05, and yielding displacement dy = 0.05m.

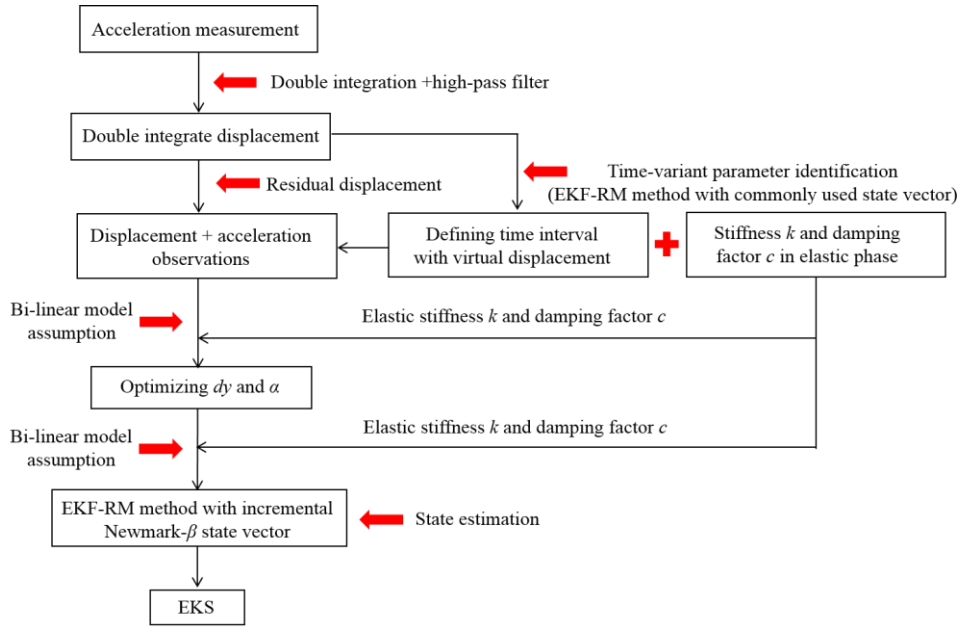

Figure 3. Flow chart of displacement estimation.

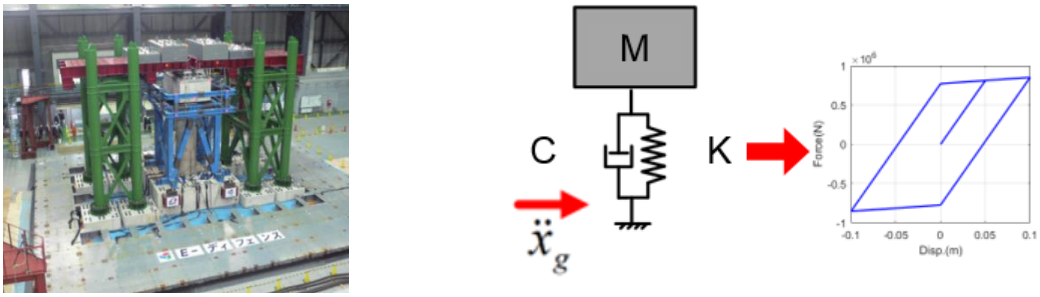

(a) (b)

Figure 4. (a) C1-1 prototype experiment structure (b) simplified bi-linear SDOF model.

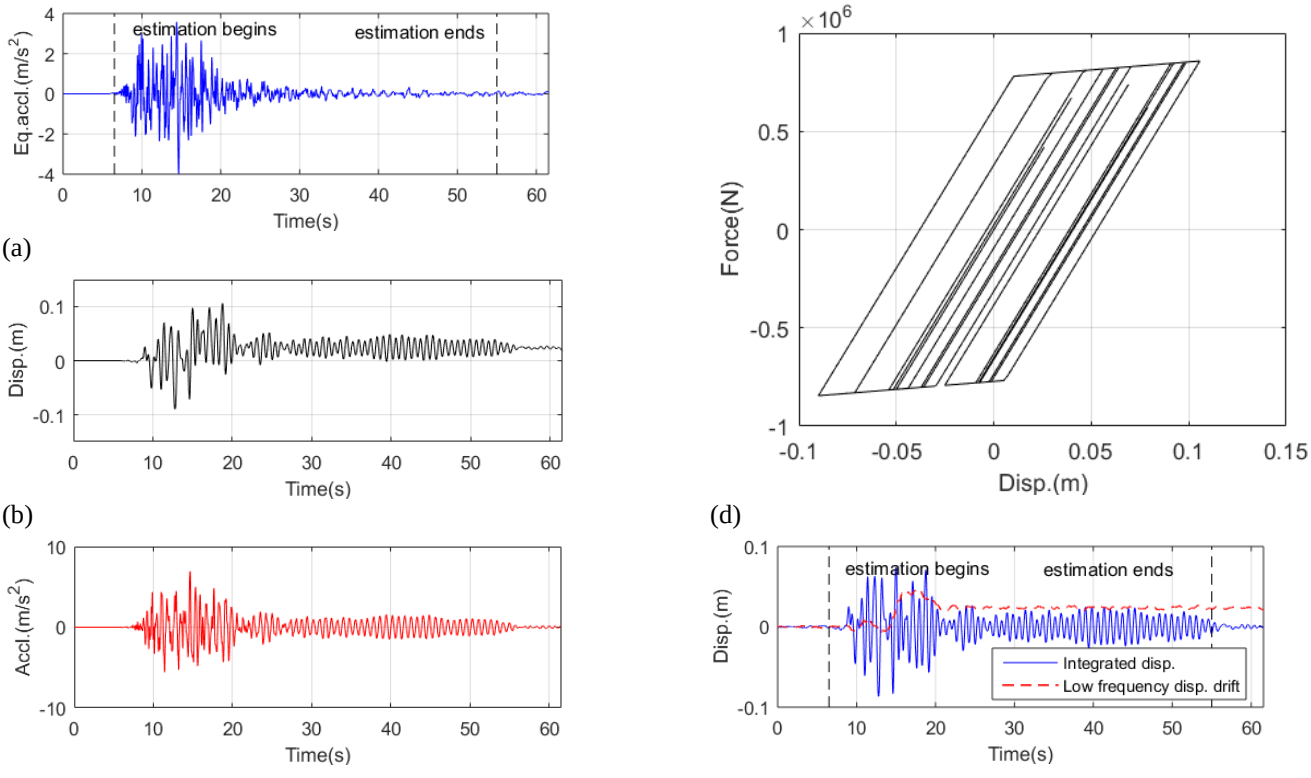

Figure 5. Bi-linear model simulation response; (a) earthquake acceleration (b) displacement (c) acceleration (d) hysteresis loop (e) double integrated displacement and low frequency drift.

The forward analysis is conduct using incremental Newmark-β method with β=1/6 and the time interval equals to 0.005s. Northridge earthquake acceleration is treated as excitation. The simulated displacement, acceleration, hysteresis loop as well as the earthquake signal is shown in Figure 5. The simulated acceleration signal is then added with white noise process whose RMS equals to 5% of that of signal (1.2m/s^2) to consider practical measurement noise. Based on the noisy acceleration, double integrated displacement is obtained by using a high-pass filter with 0.2Hz cutoff frequency. Figure 5 (e) shows the double integrated displacement and low frequency displacement drift, i.e. difference between integrated and true displacement. In this case, the residual displacement occurs from about 22s with 2.3cm. Subsequently time-variant stiffness value can be identified using the integrated displacement and acceleration. R matrix and initial Q is set as R=*diag*([10^{-5},5×10^{-3}]) and Q= *diag*([10^{-6},10^{-4},0,0]); initial parameter value and error covariance matrix are set $1.0\theta_{real}$ and *diag*([$0.1\theta_{real}$]^2) where θ_{real} stands for real elastic parameter vector. Besides, the α_Q coefficient of RM algorithm is set as 1/15. The period of time of estimation is shown in Figure 5 (a). The identified time-variant parameter time histories are shown in Figure 6. By using the integrated displacement, the time-variant parameters are identified based on normal state space model, i.e. equivalent stiffness and damping coefficient of nonlinear system are identified rather than tangential ones. Except the fluctuation during the initial time, significant stiffness reduction occurs between 4~15s which matches with the time interval of significant low frequency drift well as shown in Figure 7(a). For the latter part of the identification, e.g. after 15s, the identified parameters coincide with those true elastic parameter values well.

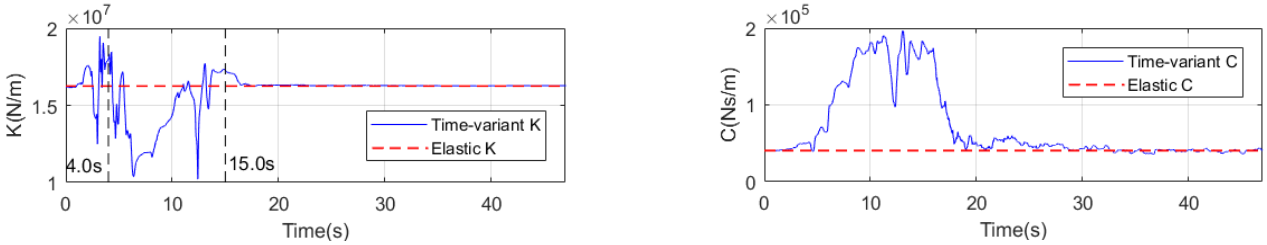

(a) (b)

Figure 6. Time-variant parameter estimation time history (a) stiffness (b) damping factor.

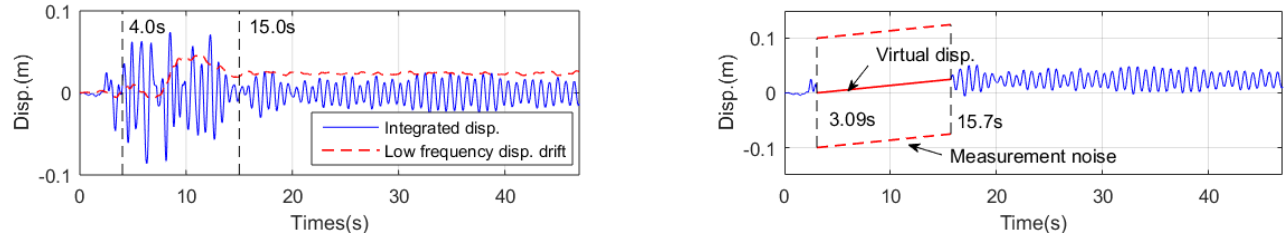

(a) (b)

Figure 7. (a) Integrated displacement (b) displacement observation.

Based on the identification results, the time interval with virtual displacement is defined from 3.09s to 15.7s. The latter part of integrated displacement is summed with residual displacement, i.e. 2.3cm. The displacement observation is shown in Figure 7(b).In this study, the measurement noise value of virtual displacement is selected based on the maximum value of integrated displacement. Specifically, 0.10m is employed in this case because the maximum value of integrated displacement is about 0.09m as shown in Figure 7(a).For the integrated displacement part, the measurement noise used in time-variant parameter identification can be applied. However, since the integrated displacement cannot match the real displacement perfectly, e.g. during the initial period of time, a relatively large noise value could be employed for the displacement component of the R matrix in order to estimate more accurate displacement result. In this case, it is selected as 0.01m. Therefore, in following displacement estimation, R matrix is set as *diag*([10^{-2},5×10^{-3}]) and *diag*([10^{-4},5×10^{-3}]) for the virtual displacement and integrated displacement part respectively. Other computation parameters remain unchanged.

The parameters to be determined is yielding displacement dy and post-yielding stiffness ratio α. In terms of the fitness function equation (18), the computation interval is set same as virtual displacement interval, i.e. 3.09s~15.7s. The genetic algorithm (GA) is applied here to find optimized values.

First of all, acceleration process noise Q_{accl} computed using true dy and α value (dy=0.05, α=0.05) and a set of wrong values (dy=0.03, α=0.03) are compared in Figure 8. The acceleration process noise corresponding to

true parameter value is indeed smaller than that of wrong parameters especially during the time interval with virtual displacement. Thus the Q_{accl} is sensitive to the two parameters, and it is reasonable to regard Q_{accl} as the fitness function for GA.

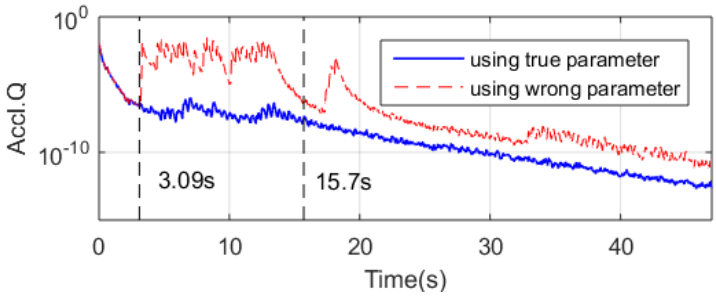

Figure 8. Comparison of acceleration process noise.

Before conducting GA, it is required to set the identification parameter ranges. Here it is proposed to define them based on the double integrated displacement. The hysteresis loop is plot in Figure 9(a). Since the true hysteresis loop here is a bi-linear model, the double integrated displacement loop is clear and close to the true loop. Parameter *dy* and α can be easily determined from the thick dashed lines in the figure. However, relatively wide ranges of parameters are defined as $0.01 \le dy \le 0.10$ and $0.03 \le \alpha \le 0.08$ based on them so as to consider more uncertain condition in practice. In the GA computation, 20 generations of30 populations are considered. The total computation time is about 20 minutes in a standard laptop PC and Figure 9(b) shows the convergence plot of GA. The optimized *dy* and α value are 0.050 and 0.0449 respectively. Based on the optimized values, the estimated displacement is shown in Figure 10.

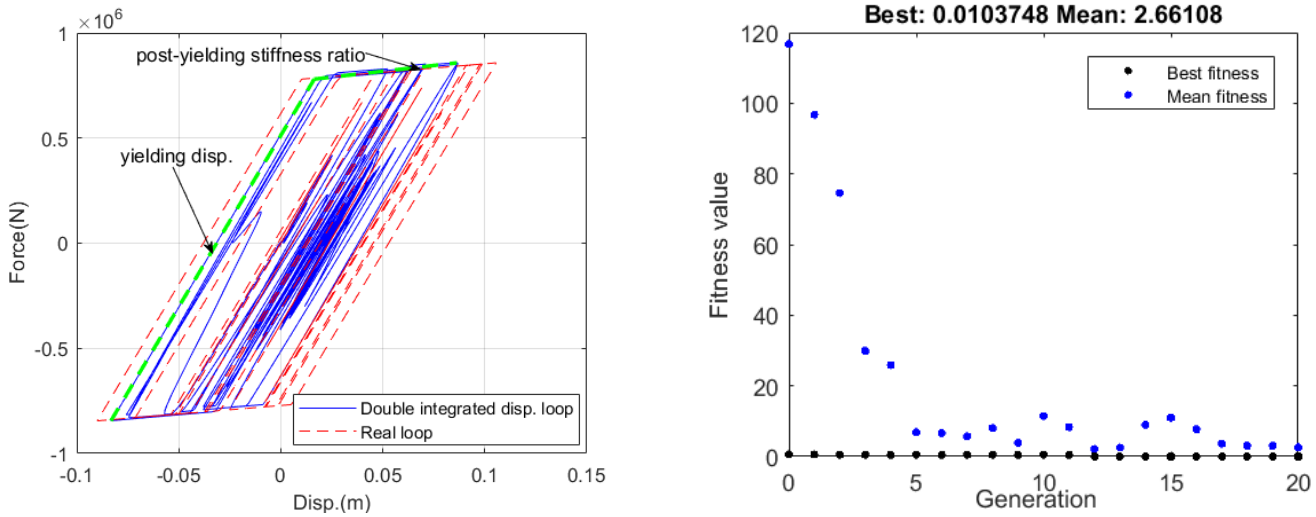

(a) (b)

Figure 9. (a) Comparison between real and double integrated displacement hysteresis loop (b) convergence plot of GA.

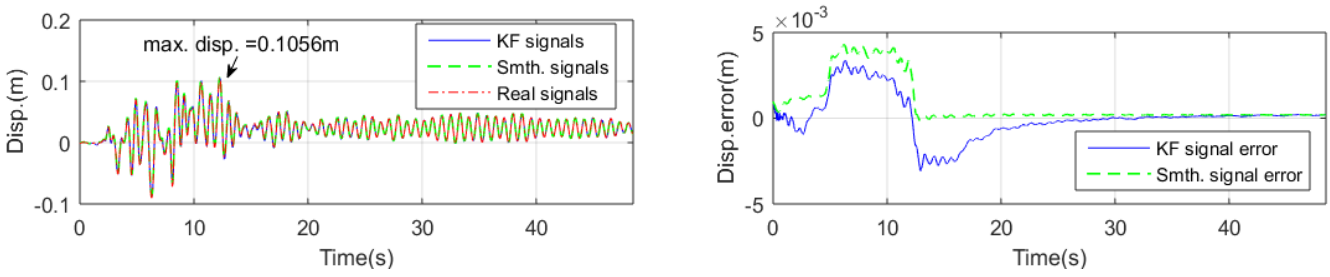

(a) (b)

Figure 10. Estimated displacement (a) comparison between estimated and real displacement (b) estimation error comparison.

Figure 10(a) shows that the estimated displacement almost coincides with the real one. In Figure 10(b), the maximum errors of EKF and EKS are both smaller than 5mm, and the errors at maximum displacement are 0.5mm and 2mmfor EKF and EKS respectively. Overall, the accuracy of EKS is higher than EKF since there is almost no error after around 12s in EKS signal.

4 EXPERIMENT VALIDATION OF THE DISPLACEMENT ESTIMATION METHOD

The C1-1 bridge pier experiment introduced in last section is employed here (ASEBI 2020).By simplifying it into a SDOF model, the displacement on the top of the pier cap is to be estimated. The equivalent concentration mass is 252.5 ton. Specifically, the north-south (NS) direction of the experiment under Takatori100%1 excitation case is analyzed here. A group of wave forms, i.e. earthquake excitation, relative displacement and relative acceleration, in the case are shown in Figure 11.The residual displacement is -1.8cm and the sampling frequency is 200Hz.

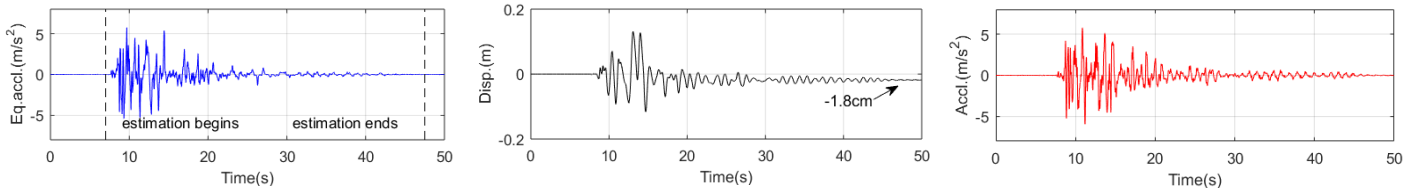

(a) (b) (c)

Figure 11. Takatori100%1 NS case (a) earthquake acceleration (b) relative displacement (c) relative acceleration.

In the first place, the acceleration is used to obtain double integrated displacement; the integrate displacement as well as corresponding low frequency drift part is presented in Figure 12 for the estimation time interval as shown in Figure 11(a). Based on the integrated displacement and acceleration, time-variant parameters of the SDOF system are identified. In this step, the R matrix and initial Q matrix is set as R= $diag$([5×10^{-6},10^{-2}]) (corresponding to displacement and acceleration measurement noise) and Q= $diag$([10^{-6},10^{-4},0,0]); the α_Q value of RM algorithm is set as 1/15. The time-variant parameter results are shown in Figure 13. Stiffness reduction period mainly occurs between 3~15s. For the latter part of the identification, i.e. after 15s, the stiffness and damping factor are stable which are about 1.28×10^{7}N/m and 3.0×10^{5}Ns/m respectively.

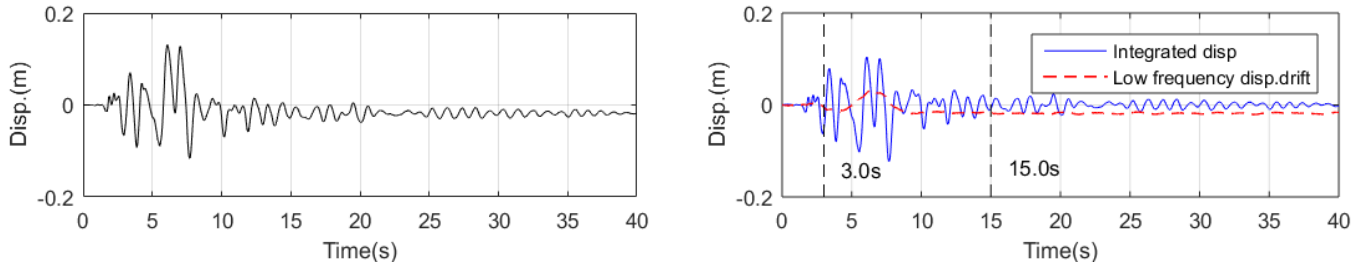

(a) (b)

Figure 12. (a) True displacement (b) double integrated displacement and low frequency drift.

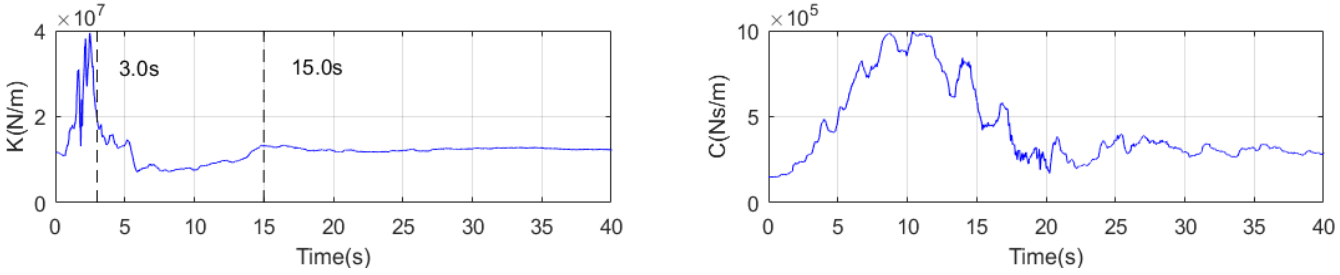

(a) (b)

Figure 13. (a) Time-variant stiffness value (b) time-variant damping factor value.

The time interval with virtual displacement is defined from 2.66s to 15.61s. Combing with residual displacement -1.8cm in the latter part, the displacement observation is established and shown in Figure 14(a). The measurement noise for the virtual displacement is set as 0.15m.In the following displacement estimation, the R matrix is set as $diag([0.0225, 10^{-2}])$ and $diag([5\times10^{-5}, 10^{-2}])$ for the virtual displacement and integrated displacement part respectively. Other computation parameters remain unchanged.

Subsequently, bi-linear model parameter dy and α are optimized using GA. The range of them is defined based on the thick dashed line in Figure 14(b). Here, the range is defined as $0.02 \leqslant dy \leqslant 0.05$ and $0.3 \leqslant \alpha \leqslant 0.8$ and the final optimized dy and α values are 0.0492 and 0.5136 respectively. Based on these values, the displacement is estimated which is shown in Figure 15. Since the hysteresis loop is not close to bi-linear model, the result from EKF is actually not accurate, i.e. maximum error is about 6cm; however, by applying the EKS, the estimate displacement becomes much more accurate in which the maximum error is only about 9mm.

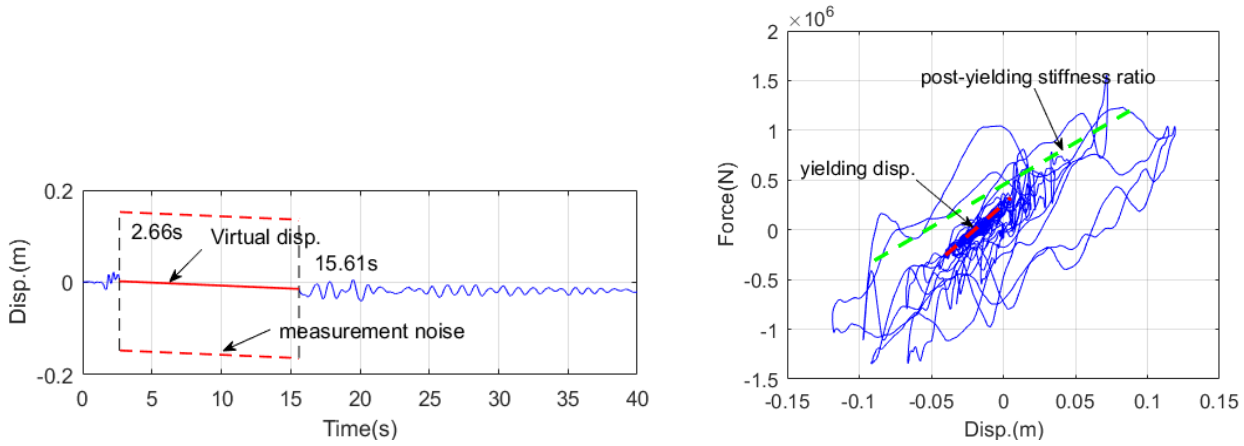

(a) (b)

Figure 14. (a) Displacement observation (b) hysteresis loop of double integrated displacement.

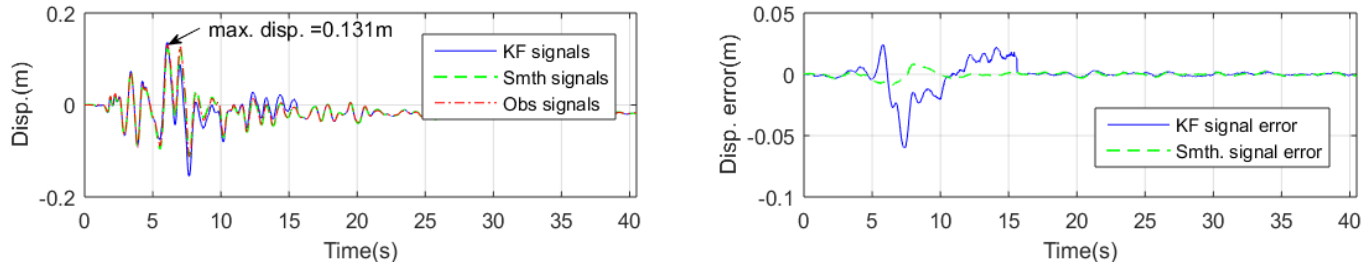

(a) (b)

Figure 15. Displacement estimation results of Takatori100%1 NS case (a) estimated displacement (b) displacement error.

5 CONCLUSIONS

In this paper, a displacement estimation method is proposed for nonlinear SDOF system under seismic excitation using EKF and parameter optimization. With acceleration measurement, double integrated displacement, and residual displacement value regarded as known, displacement signal during significant system nonlinearity is estimated assuming a bi-linear hysteresis model in EKF and further smoothed using EKS. The effectiveness of the proposed method is verified through a numerical bi-linear SDOF model and a bridge pier experiment. The estimated displacements present good accuracies.

REFERENCES

Chatzis, M.N., E.N. Chatzi, and A.W. Smyth, *An experimental validation of time domain system identification methods with fusion of heterogeneous data.* Earthquake Engineering & Structural Dynamics, 2015. 44(4): p. 523-547.

Chatzi, E.N. and C. Fuggini, *Online correction of drift in structural identification using artificial white noise observations and an unscented Kalman filter.* Smart Struct. Syst, 2015. 16(2): p. 295-328.

Kawashima, K., G.A. MacRae, J. Hoshikuma, et al., *Residual displacement response spectrum*. Journal of Structural Engineering, 1998.124(5): p. 523-530.

Kuleli, M. and T. Nagayama, *A robust structural parameter estimation method using seismic response measurements.* Structural Control and Health Monitoring, 2020. 27(3): p. e2475.
Kuleli, M., *Stiffness condition assessment of bridge lateral resisting systems with unscented Kalman filter using seismic acceleration response measurements*, in *Department of Civil Engineering*. 2018, The University of Tokyo.
Lee, H.S., Y.H. Hong, and H.W. Park, *Design of an FIR filter for the displacement reconstruction using measured acceleration in low‐frequency dominant structures.* International Journal for Numerical Methods in Engineering, 2010. 82(4): p. 403-434.
Nagayama, T., C. Zhang, *A numerical study on bridge deflection estimation using multi-channel acceleration measurement*. Journal of Structural Engineering A, JSCE, 2017. 63A: p.209-215.
Park, J.-W., S.-H. Sim, and H.-J. Jung, *Development of a wireless displacement measurement system using acceleration responses.* Sensors, 2013. 13(7): p. 8377-8392.
Rauch, H.E., F. Tung, and C.T. Striebel, *Maximum likelihood estimates of linear dynamic systems.* AIAA journal, 1965. 3(8): p. 1445-1450.
Robbins, H. and S. Monro, *A Stochastic Approximation Method.* Ann. Math. Statist., 1951. 22(3): p. 400-407.
Shodja, A.H. and F.R. Rofooei, *Using a lumped mass, nonuniform stiffness beam model to obtain the interstory drift spectra.* Journal of Structural Engineering, 2014. 140(5): p. 04013109.
Skolnik, D.A. and J.W. Wallace, *Critical assessment of interstory drift measurements.* Journal of structural engineering, 2010. 136(12): p. 1574-1584.
Technical Report for Large-scale Shaking Table Experiment on a Component Model (C1-1model) Using E-Defense, Experiment on a RC Column Build in 1970s which Fails in Flexure, in, National Research Institute for Earth Science and Disaster Resilience, [ASEBI] https://www.edgrid.jp
Yang, J., J. Li, and G. Lin, *A simple approach to integration of acceleration data for dynamic soil–structure interaction analysis.* Soil dynamics and earthquake engineering, 2006. 26(8): p. 725-734.